

Semileptonic $B_{(s)}$ meson decays to

$D_0^*(2300)$, $D_{s0}^*(2317)$, $D_{s1}(2460)$, $D_{s1}(2536)$, $D_1(2420)$ and $D_1(2430)$

within the covariant light-front approach

You-Ya Yang,¹ Zhi-Qing Zhang,^{1,*} and Hao Yang¹

¹ *School of Physics, Henan University of Technology, Zhengzhou, Henan 450001, China*

(Dated: January 16, 2025)

Abstract

In this work, we investigate the semileptonic decays of $B_{(s)}$ meson to $D_0^*(2300)$, $D_{s0}^*(2317)$, $D_{s1}(2460)$, $D_{s1}(2536)$, $D_1(2420)$ and $D_1(2430)$ in the covariant light-front quark model (CLFQM). We combine the helicity amplitudes via the corresponding form factors to obtain the branching ratios of the semileptonic decays $B_{(s)} \rightarrow D_{(s)}^{**} \ell \nu_\ell$ with $D_{(s)}^{**}$ referring to a P-wave excited charmed meson $D_0^*(2300)$, $D_{s0}^*(2317)$, $D_{s1}(2460)$, $D_{s1}(2536)$, $D_1(2420)$ or $D_1(2430)$ and $\ell = e, \mu, \tau$. Furthermore, we also take into account another two physical observables, namely the longitudinal polarization fraction f_L and the forward-backward asymmetry A_{FB} . Most of our predictions are comparable to the results given by other theoretical approaches and the present available data. The branching ratios of the semileptonic decay channels $B_s \rightarrow D_{s1}(2460) \ell \nu_\ell$ and $B \rightarrow D_1(2420) \ell \nu_\ell$ are larger than those of the semileptonic decays $B_s \rightarrow D_{s1}(2536) \ell \nu_\ell$ and $B \rightarrow D_1(2430) \ell \nu_\ell$, respectively. We find that the long-standing '1/2 vs 3/2 puzzle' in the decays $B^+ \rightarrow \bar{D}_1^{(\prime)0} \ell'^+ \nu_{\ell'}$ ($\ell' = e, \mu$) can be solved by taking some negative mixing angle θ_s values within a range from -30.3° to -24.9° , corresponding to θ of about $5^\circ \sim 10.4^\circ$. While Belle collaboration updated their measurements for the decays $B^0 \rightarrow D_0^{*-} \ell'^+ \nu_{\ell'}$ with only a small upper limit $Br(B^0 \rightarrow D_0^{*-} \ell'^+ \nu_{\ell'}) < 0.44 \times 10^{-3}$ obtained, which is much larger than most theoretical predictions and causes a new puzzle.

PACS numbers: 13.25.Hw, 12.38.Bx, 14.40.Nd

* zhangzhiqing@haut.edu.cn (corresponding author)

I. INTRODUCTION

In the conventional quark model, these P-wave orbitally excited charmed mesons $D_0^*(2300)$, $D_{s0}^*(2317)$, $D_{s1}(2460)$, $D_{s1}(2536)$, $D_1(2420)$ and $D_1(2430)$ can be view as constituent quark-antiquark pairs. They are usually classified according to the quantum numbers $(^{2S+1})L_J$: the scalar mesons $D_0^*(2300)$ and $D_{s0}^*(2317)$ correspond to 3P_0 . While there exist two different kinds of axial-vector mesons, namely 1P_1 and 3P_1 , which can undergo mixing when the two constituent quarks are different. In the heavy quark limit, the heavy quark spin and the total angular momentum of the light quark are good quantum numbers, it is more convenient to use the L_J^j configurations¹ to classify them: the scalar mesons $D_0^*(2300)$ and $D_{s0}^*(2317)$ belong to $P_0^{1/2}$, $D_1(2430)(D_{s1}(2536))$ and $D_1(2420)(D_{s1}(2460))$ correspond to $P_1^{3/2}$ and $P_1^{1/2}$, respectively. However, beyond the heavy quark limit, there is a mixing between $P_1^{3/2}$ and $P_1^{1/2}$, denoted by $D_1^{3/2}$ and $D_1^{1/2}$, respectively², that is

$$\begin{aligned} |D_1(2420)\rangle &= |D_1^{1/2}\rangle \sin \theta_s + |D_1^{3/2}\rangle \cos \theta_s, \\ |D_1(2430)\rangle &= -|D_1^{3/2}\rangle \sin \theta_s + |D_1^{1/2}\rangle \cos \theta_s. \end{aligned} \quad (1)$$

While the states $D_1^{1/2}$ and $D_1^{3/2}$ are expected to be a mixture of states 1P_1 and 3P_1 denoted by 1D_1 and 3D_1 , respectively,

$$\begin{aligned} |D_1^{3/2}\rangle &= \sqrt{\frac{2}{3}}|^1D_1\rangle + \sqrt{\frac{1}{3}}|^3D_1\rangle, \\ |D_1^{1/2}\rangle &= -\sqrt{\frac{1}{3}}|^1D_1\rangle + \sqrt{\frac{2}{3}}|^3D_1\rangle. \end{aligned} \quad (2)$$

Combining Eq. (1) and Eq. (2), one can find that the physical states $D_1(2420)$ and $D_1(2430)$ can be written as

$$\begin{aligned} |D_1(2420)\rangle &= |^1D_1\rangle \cos \theta + |^3D_1\rangle \sin \theta, \\ |D_1(2430)\rangle &= -|^1D_1\rangle \sin \theta + |^3D_1\rangle \cos \theta. \end{aligned} \quad (3)$$

where $\theta_s = 7^\circ$ and $\theta = \theta_s + 35.3^\circ$ [1]. There exist many puzzles in these several P-wave excited states, such as the low mass puzzle for the states $D_0^*(2300)$, $D_{s0}^*(2317)$ and $D_{s1}(2460)$ [2–5], the SU(3) mass hierarchy puzzle between $D_0^*(2300)$ and $D_{s0}^*(2317)$, large width difference between them [6], especially, the long-standing ‘1/2 vs 3/2 puzzle’ [7–10], that is the theoretical predictions for the branching ratios of semileptonic B decays

¹ $j(L)$ being the total (orbital) angular momentum of the light quark.

² Here we take the physical states $D_1(2430)$ and $D_1(2420)$ as an example to explain, it is similar to the states $D_{s1}(2536)$ and $D_{s1}(2460)$.

into $D^{1/2+}$ are much smaller than those into $D^{3/2+}$, which conflicts with the experimental measurements [2, 4, 11]. These unexpected disparities between theory and experiment have sparked many explanations about their inner structures, such as the molecular states, the compact tetraquark states, the states of $\bar{c}s$ mixed with four-quark states, and so on [12–27].

In this paper we investigate the semileptonic $B_{(s)}$ meson decays to $D_0^*(2300)$, $D_{s0}^*(2317)$, $D_{s1}(2460)$, $D_{s1}(2536)$, $D_1(2420)$ and $D_1(2430)$ by using the covariant light-front quark model (CLFQM). For the semileptonic decays, the hadronic transition matrix element between the initial and final mesons is most crucial for theoretical calculations, which can be characterized by several form factors. The form factors can be extracted from data or relied on some non-perturbative methods. The $B_{(s)} \rightarrow D_{(s)}^{**}$ transition form factors were initially calculated in the improved version of the Isgur-Scora-Ginsein-Wise (ISGW) quark model, the so-called ISGW2 [28]. Some of them were calculated using the CLFQM [29], QCD sum rules (QCDSR) [30–32] and light-cone sum rules (LCSRs) [6]. Additionally, with the available experimental data as inputs, the form factors of the $B_{(s)}$ to these excited charmed meson transitions and the corresponding semileptonic decays were also investigated based on the heavy quark effective theory (HQET), including the next-to-leading order corrections of heavy quark expansion and new physics (NP) effects [33–36]. As one of the popular non-perturbative methods, the CLFQM has been used successfully to study the form factors [29, 37–40]. Based on the form factors and helicity formalisms, we also calculate another two physical observables: the forward-backward asymmetry A_{FB} and the longitudinal polarization fraction f_L , respectively.

The arrangement of this paper is as follows: In Section II, the formalism of the CLFQM, the hadronic matrix elements and the helicity amplitudes combined via form factors are presented. The numerical results for the $B_{(s)}$ meson to $D_0^*(2300)$, $D_{s0}^*(2317)$, $D_{s1}(2460)$, $D_{s1}(2536)$, $D_1(2420)$ and $D_1(2430)$ transition form factors, the branching ratios, the forward-backward asymmetries A_{FB} and the longitudinal polarization fractions f_L for the corresponding decays are presented in Section III. In addition, the detailed numerical analysis and discussion, including comparisons with the data and other model calculations, are carried out. The conclusions are presented in the final part.

II. FORMALISM

A. The covariant light-front quark model

Under the covariant light-front quark model, the light-front coordinates of a momentum p are defined as $p = (p^-, p^+, p_\perp)$ with $p^\pm = p^0 \pm p_z$ and $p^2 = p^+ p^- - p_\perp^2$. If the momenta of the quark and antiquark with masses $m_1^{(\prime\prime)}$ and m_2 in the incoming (outgoing) meson are denoted as $p_1^{(\prime\prime)}$ and p_2 , respectively, the momentum of the incoming (outgoing) meson with mass $M'(M'')$ can be written as $P' = p_1' + p_2$ ($P'' = p_1'' + p_2$). Here, we use the same notation as those in Refs. [29, 41] and M' refers to m_B for B meson decays. These momenta can be related each other through the internal variables (x_i, p'_\perp)

$$p_{1,2}^{\prime+} = x_{1,2} P'^+, \quad p_{1,2\perp}' = x_{1,2} P'_\perp \pm p'_\perp, \quad (4)$$

with $x_1 + x_2 = 1$. Using these internal variables, we can define some quantities for the incoming meson which will be used in the following calculations

$$\begin{aligned} M_0'^2 &= (e_1' + e_2)^2 = \frac{p_\perp'^2 + m_1'^2}{x_1} + \frac{p_\perp^2 + m_2^2}{x_2}, \quad \widetilde{M}_0' = \sqrt{M_0'^2 - (m_1' - m_2)^2}, \\ e_i^{(\prime)} &= \sqrt{m_i^{(\prime)2} + p_\perp'^2 + p_z'^2}, \quad p_z' = \frac{x_2 M_0'}{2} - \frac{m_2^2 + p_\perp'^2}{2x_2 M_0'}, \end{aligned} \quad (5)$$

where the kinetic invariant mass of the incoming meson M_0' can be expressed as the energies of the quark and the antiquark $e_i^{(\prime)}$. It is similar to the case of the outgoing meson.

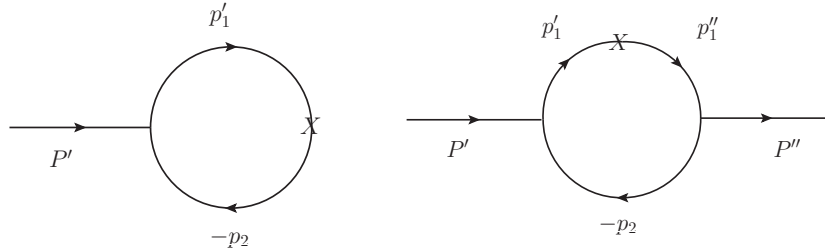


FIG. 1: Feynman diagrams for $B_{(s)}$ decay (left) and transition (right) amplitudes, where $P^{(\prime\prime)}$ is the incoming (outgoing) meson momentum, $p_1^{(\prime\prime)}$ is the quark momentum and p_2 is the antiquark momentum. The X in the diagrams denotes the vector or axial-vector transition vertex.

To calculate the amplitudes for the transition form factors, we need the Feynman rules

for the meson-quark-antiquark vertices $i\Gamma'_M$ ³, which are listed as

$$i\Gamma'_{D_0^*} = -iH'_{D_0^*}, \quad (6)$$

$$i\Gamma'_{^3D_1} = -iH'_{^3D_1} \left[\gamma_\mu + \frac{1}{W'_{^3D_1}} (p'_1 - p_2)_\mu \right] \gamma_5, \quad (7)$$

$$i\Gamma'_{^1D_1} = -iH'_{^1D_1} \left[\frac{1}{W'_{^1D_1}} (p'_1 - p_2)_\mu \right] \gamma_5. \quad (8)$$

The form factors of the transitions $B \rightarrow D_0^*$ and $B \rightarrow ^iD_1 (i = 1, 3)$ induced by the vector and axial-vector currents are defined as

$$\langle D_0^*(P'') | A_\mu | B(P') \rangle = i [u_+(q^2)P_\mu + u_-(q^2)q_\mu], \quad (9)$$

$$\langle ^iD_1(P'', \varepsilon) | A_\mu | B(P') \rangle = -q(q^2)\epsilon_{\mu\nu\alpha\beta}\varepsilon^{*\nu}P^\alpha q^\beta, \quad (10)$$

$$\langle ^iD_1(P'', \varepsilon) | V_\mu | B(P') \rangle = i \{ l(q^2)\varepsilon_\mu^* + \varepsilon^* \cdot P [P_\mu c_+(q^2) + q_\mu c_-(q^2)] \}. \quad (11)$$

In calculations, the Bauer-Stech-Wirbel (BSW) [42] transition form factors are more frequently used and defined by

$$\langle D_0^*(P'') | A_\mu | B(P') \rangle = \left(P_\mu - \frac{m_B^2 - m_{D_0^*}^2}{q^2} q_\mu \right) F_1^{BD_0^*}(q^2) + \frac{m_B^2 - m_{D_0^*}^2}{q^2} q_\mu F_0^{BD_0^*}(q^2), \quad (12)$$

$$\begin{aligned} \langle ^iD_1(P'', \varepsilon^{\mu*}) | V_\mu | B(P') \rangle = & -i \left\{ (m_B - m_{^iD_1}) \varepsilon_\mu^* V_1^{B^iD_1}(q^2) - \frac{\varepsilon^* \cdot P}{m_B - m_{^iD_1}} P_\mu V_2^{B^iD_1}(q^2) \right. \\ & \left. - 2m_{^iD_1} \frac{\varepsilon^* \cdot P}{q^2} q_\mu [V_3^{B^iD_1}(q^2) - V_0^{B^iD_1}(q^2)] \right\}, \end{aligned} \quad (13)$$

$$\langle ^iD_1(P'', \varepsilon^{\mu*}) | A_\mu | B(P') \rangle = -\frac{1}{m_B - m_{^iD_1}} \epsilon_{\mu\nu\alpha\beta} \varepsilon^{*\nu} P^\alpha q^\beta A^{B^iD_1}(q^2), \quad (14)$$

where $P = P' + P''$, $q = P' - P''$ and the convention $\epsilon_{0123} = 1$ is adopted.

To smear the singularity at $q^2 = 0$ in Eq. (13), the following relations are required

$$V_3^{B^iD_1}(0) = V_0^{B^iD_1}(0), \quad (15)$$

$$V_3^{B^iD_1}(q^2) = \frac{m_B - m_{^iD_1}}{2m_{^iD_1}} V_1^{B^iD_1}(q^2) - \frac{m_B + m_{^iD_1}}{2m_{^iD_1}} V_2^{B^iD_1}(q^2). \quad (16)$$

³ In the following we take the transitions $B \rightarrow D_0^*$ and $B \rightarrow ^3D_1, ^1D_1$ as examples. It is similar for the transitions $B_s \rightarrow D_{s0}^*$ and $B_s \rightarrow ^3D_{s1}, ^1D_{s1}$. From now on, we will use $D_0^*, D_{s0}^*, D_{s1}, D'_{s1}, D_1$ and D'_1 to represent $D_0^*(2300), D_{s0}^*(2317), D_{s1}(2460), D_{s1}(2536), D_1(2420)$ and $D_1(2430)$, respectively, for simplicity.

These two kinds of form factors are related to each other via

$$F_1^{BD^*}(q^2) = -u_+(q^2), F_0^{BD^*}(q^2) = -u_+(q^2) - \frac{q^2}{q \cdot P} u_-(q^2), \quad (17)$$

$$A^{B \ ^iD_1}(q^2) = -(m_B - m_{iD_1})q(q^2), V_1^{B \ ^iD_1}(q^2) = -\frac{l(q^2)}{m_B - m_{iD_1}}, \quad (18)$$

$$V_2^{B \ ^iD_1}(q^2) = (m_B - m_{iD_1})c_+(q^2), V_3^{B \ ^iD_1}(q^2) - V_0^{B \ ^iD_{s1}}(q^2) = \frac{q^2}{2m_{iD_1}}c_-(q^2). \quad (19)$$

For the general $B \rightarrow M$ transitions with M being a scalar or axial-vector meson, the decay amplitude at the lowest order is [43]

$$\mathcal{M}^{BM} = -i^3 \frac{N_c}{(2\pi)^4} \int d^4 p'_1 \frac{H'_B (H''_M)}{N'_1 N''_1 N_2} S_\mu^{BM}, \quad (20)$$

where $N_1^{l(n)} = p_1^{l(n)2} - m_1^{l(n)2}$ and $N_2 = p_2^2 - m_2^2$ arise from the quark propagators. For our considered transitions $B \rightarrow D_0^*$ and $B \rightarrow \ ^1D_1, \ ^3D_1$, the traces $S_\mu^{BD_0^*}, S_{\mu\nu}^{B \ ^1D_1}$ and $S_{\mu\nu}^{B \ ^3D_1}$ can be directly written out by using the Lorentz contraction as follows

$$S_\mu^{BD_0^*} = \text{Tr} [(\not{p}'_1 + m''_1) \gamma_\mu \gamma_5 (\not{p}'_1 + m'_1) \gamma_5 (-\not{p}_2 + m_2)], \quad (21)$$

$$\begin{aligned} S_{\mu\nu}^{B \ ^1D_1} &= \left(S_V^{B \ ^1D_1} - S_A^{B \ ^1D_1} \right)_{\mu\nu} \\ &= \text{Tr} \left[\left(-\frac{1}{W''_{1D_1}} (p''_1 - p_2)_\nu \right) \gamma_5 (\not{p}'_1 + m''_1) (\gamma_\mu - \gamma_\mu \gamma_5) (\not{p}'_1 + m'_1) \gamma_5 (-\not{p}_2 + m_2) \right], \end{aligned} \quad (22)$$

$$\begin{aligned} S_{\mu\nu}^{B \ ^3D_1} &= \left(S_V^{B \ ^3D_1} - S_A^{B \ ^3D_1} \right)_{\mu\nu} \\ &= \text{Tr} \left[\left(\gamma_\nu - \frac{1}{W''_{3D_1}} (p''_1 - p_2)_\nu \right) \gamma_5 (\not{p}'_1 + m''_1) (\gamma_\mu - \gamma_\mu \gamma_5) (\not{p}'_1 + m'_1) \gamma_5 (-\not{p}_2 + m_2) \right]. \end{aligned} \quad (23)$$

The form factors can be obtained by matching the coefficients listed in Eqs. (9)-(11) with the corresponding amplitudes given Eq. (20). The specific expressions for these transition form factors are collected in Appendix B. It is noticed that the form factors of the transitions $B \rightarrow D_1$ and $B \rightarrow D'_1$ can be obtained from those of the transitions $B \rightarrow \ ^1D_1$ and $B \rightarrow \ ^3D_1$ through Eq. (3).

B. Wave functions and decay constants

The light-front wave functions (LFWFs) are needed in the form factor calculations. Although the LFWFs can be derived from solving the relativistic Schrödinger equation theoretically, it is difficult to obtain their exact solutions in many cases. Consequently,

we will use the phenomenological Gaussian-type wave functions in this work,

$$\begin{aligned}\varphi' &= \varphi'(x_2, p'_\perp) = 4 \left(\frac{\pi}{\beta'^2} \right)^{\frac{3}{4}} \sqrt{\frac{dp'_z}{dx_2}} \exp\left(-\frac{p'^2_z + p'^2_\perp}{2\beta'^2}\right), \\ \varphi'_p &= \varphi'_p(x_2, p'_\perp) = \sqrt{\frac{2}{\beta'^2}} \varphi', \quad \frac{dp'_z}{dx_2} = \frac{e'_1 e_2}{x_1 x_2 M'_0},\end{aligned}\quad (24)$$

where the parameter β' describes the momentum distribution and is approximately of order Λ_{QCD} . It can be usually determined by the decay constants through the following analytic expressions [29, 41],

$$f_{D_0^*} = \frac{N_c}{16\pi^3} \int dx_2 d^2 p'_\perp \frac{h'_{D_0^*}}{x_1 x_2 (M'^2 - M_0'^2)} 4(m'_1 x_2 - m_2 x_1), \quad (25)$$

$$\begin{aligned}f^{3D_1} &= -\frac{N_c}{4\pi^3 M'} \int dx_2 d^2 p'_\perp \frac{h'_{3D_1}}{x_1 x_2 (M'^2 - M_0'^2)} \\ &\times \left[x_1 M_0'^2 - m'_1 (m'_1 + m_2) - p'^2_\perp - \frac{m'_1 - m_2}{w'_{3D_1}} p'^2_\perp \right],\end{aligned}\quad (26)$$

$$f_{1D_1} = \frac{N_c}{4\pi^3 M'} \int dx_2 d^2 p'_\perp \frac{h'_{1D_1}}{x_1 x_2 (M'^2 - M_0'^2)} \left(\frac{m'_1 - m_2}{w'_{1D_1}} p'^2_\perp \right), \quad (27)$$

where m'_1 and m_2 represent the constituent quarks of the states D_0^* , 3D_1 and 1D_1 . The decay constants can be obtained through experimental measurements for the purely leptonic decays or theoretical calculations. The explicit forms of h'_M are given by [43]

$$h'_{D_0^*} = \sqrt{\frac{2}{3}} h'_{3D_1} = (M'^2 - M_0'^2) \sqrt{\frac{x_1 x_2}{N_c}} \frac{1}{\sqrt{2} \widetilde{M}'_0} \frac{\widetilde{M}'_0{}^2}{2\sqrt{3} M'_0} \varphi'_p, \quad (28)$$

$$h'_{1D_1} = (M'^2 - M_0'^2) \sqrt{\frac{x_1 x_2}{N_c}} \frac{1}{\sqrt{2} \widetilde{M}'_0} \varphi'_p. \quad (29)$$

C. Helicity amplitudes and observables

Since the form factors involving the fitted parameters for most of the transitions $B_{(s)} \rightarrow D_{(s)}^{**}$ have been investigated in our recent work [44], so it is convenient to obtain the differential decay widths of these semileptonic B decays by the combination of the helicity amplitudes via form factors, which are listed as following

$$\begin{aligned}\frac{d\Gamma(B \rightarrow D_0^* \ell \nu_\ell)}{dq^2} &= \left(\frac{q^2 - m_\ell^2}{q^2} \right)^2 \frac{\sqrt{\lambda(m_B^2, m_{D_0^*}^2, q^2)} G_F^2 |V_{cb}|^2}{384 m_B^3 \pi^3} \times \frac{1}{q^2} \\ &\times \left\{ (m_\ell^2 + 2q^2) \lambda(m_B^2, m_{D_0^*}^2, q^2) F_1^2(q^2) + 3m_\ell^2 (m_B^2 - m_{D_0^*}^2)^2 F_0^2(q^2) \right\},\end{aligned}\quad (30)$$

$$\frac{d\Gamma_L(B \rightarrow D_1^{(\prime)} \ell \nu_\ell)}{dq^2} = \left(\frac{q^2 - m_\ell^2}{q^2}\right)^2 \frac{\sqrt{\lambda(m_B^2, m_{D_1^{(\prime)}}^2, q^2)} G_F^2 |V_{cb}|^2}{384 m_B^3 \pi^3} \times \frac{1}{q^2} \left\{ 3m_\ell^2 \lambda(m_B^2, m_{D_1^{(\prime)}}^2, q^2) V_0^2(q^2) + (m_\ell^2 + 2q^2) \right. \\ \left. \times \left| \frac{1}{2m_{D_1^{(\prime)}}} \left[(m_B^2 - m_{D_1^{(\prime)}}^2 - q^2)(m_B - m_{D_1^{(\prime)}}) V_1(q^2) - \frac{\lambda(m_B^2, m_{D_1^{(\prime)}}^2, q^2)}{m_B - m_{D_1^{(\prime)}}} V_2(q^2) \right] \right|^2 \right\}, \quad (31)$$

$$\frac{d\Gamma_\pm(B \rightarrow D_1^{(\prime)} \ell \nu_\ell)}{dq^2} = \left(\frac{q^2 - m_\ell^2}{q^2}\right)^2 \frac{\sqrt{\lambda(m_B^2, m_{D_1^{(\prime)}}^2, q^2)} G_F^2 |V_{cb}|^2}{384 m_B^3 \pi^3} \\ \times \left\{ (m_\ell^2 + 2q^2) \lambda(m_B^2, m_{D_1^{(\prime)}}^2, q^2) \left| \frac{A(q^2)}{m_B - m_{D_1^{(\prime)}}} \mp \frac{(m_B - m_{D_1^{(\prime)}}) V_1(q^2)}{\sqrt{\lambda(m_B^2, m_{D_1^{(\prime)}}^2, q^2)}} \right|^2 \right\}, \quad (32)$$

where $\lambda(a, b, c) = (a + b - c)^2 - 4ab$ and m_ℓ is the mass of the lepton ℓ with $\ell = e, \mu, \tau$ ⁴. The helicity amplitudes for the decays $B_s \rightarrow D_{s0}^* \ell \nu_\ell$ and $B_s \rightarrow D_{s1}^{(\prime)} \ell \nu_\ell$ can be obtained from Eqs. (30), (31) and (32), respectively, with simple replacement. The combined transverse and total differential decay widths are defined as

$$\frac{d\Gamma_T}{dq^2} = \frac{d\Gamma_+}{dq^2} + \frac{d\Gamma_-}{dq^2}, \quad \frac{d\Gamma}{dq^2} = \frac{d\Gamma_L}{dq^2} + \frac{d\Gamma_T}{dq^2}. \quad (33)$$

For the decays with $D_1^{(\prime)}$ and $D_{s1}^{(\prime)}$ involved, it is meaningful to define the polarization fraction due to the existence of different polarizations

$$f_L = \frac{\Gamma_L}{\Gamma_L + \Gamma_+ + \Gamma_-}. \quad (34)$$

As to the forward-backward asymmetry, the analytical expression is defined as [45],

$$A_{FB} = \frac{\int_0^1 \frac{d\Gamma}{d\cos\theta} d\cos\theta - \int_{-1}^0 \frac{d\Gamma}{d\cos\theta} d\cos\theta}{\int_{-1}^1 \frac{d\Gamma}{d\cos\theta} d\cos\theta} = \frac{\int b_\theta(q^2) dq^2}{\Gamma_{B \rightarrow D^{**} \ell \nu_\ell}}, \quad (35)$$

where θ is the angle between the 3-momenta of the lepton ℓ and the initial B meson in the $\ell \nu$ rest frame. The angular coefficient $b_\theta(q^2)$ for the decays $B \rightarrow D_0^* \ell \nu_\ell$ is given as [45]

$$b_\theta(q^2) = \frac{G_F^2 |V_{cb}|^2}{128 \pi^3 m_B^3} q^2 \sqrt{\lambda(q^2)} \left(1 - \frac{m_\ell^2}{q^2}\right)^2 \frac{m_\ell^2}{q^2} (H_{V,0}^s H_{V,t}^s), \quad (36)$$

with the helicity amplitudes

$$H_{V,0}^s(q^2) = \sqrt{\frac{\lambda(q^2)}{q^2}} F_1(q^2), \quad H_{V,t}^s(q^2) = \frac{m_B^2 - m_{D_0^*}^2}{\sqrt{q^2}} F_0(q^2). \quad (37)$$

⁴ For now on, we will use ℓ to represent e, μ, τ and use ℓ' to represent e, μ for simplicity.

Here $\lambda(q^2) = ((m_B - m_{D_0^*})^2 - q^2)((m_B + m_{D_0^*})^2 - q^2)$. While for the decays $B \rightarrow D_1^{(\prime)} \ell \nu_\ell$, the function $b_\theta(q^2)$ is written as

$$b_\theta(q^2) = \frac{G_F^2 |V_{cb}|^2}{128\pi^3 m_B^3} q^2 \sqrt{\lambda(q^2)} \left(1 - \frac{m_\ell^2}{q^2}\right)^2 \left[\frac{1}{2}(H_{V,+}^2 - H_{V,-}^2) + \frac{m_\ell^2}{q^2}(H_{V,0}H_{V,t}) \right], \quad (38)$$

where the corresponding helicity amplitudes are listed as

$$\begin{aligned} H_{V,\pm}(q^2) &= (m_{B_s} - m_{D_1}) V_1(q^2) \mp \frac{\sqrt{\lambda(q^2)}}{m_B - m_{D_1}} A(q^2), \\ H_{V,0}(q^2) &= \frac{m_B - m_{D_1}}{2m_{D_1} \sqrt{q^2}} \left[-(m_B^2 - m_{D_1}^2 - q^2) V_1(q^2) + \frac{\lambda(q^2) V_2(q^2)}{(m_B - m_{D_1})^2} \right], \\ H_{V,t}(q^2) &= -\sqrt{\frac{\lambda(q^2)}{q^2}} V_0(q^2), \end{aligned} \quad (39)$$

It is noticed that the subscript V in each helicity amplitude refers to the $\gamma_\mu(1-\gamma_5)$ current.

III. NUMERICAL RESULTS AND DISCUSSIONS

TABLE I: The values of the input parameters [46–50].

Mass(GeV)	$m_b = 4.8$	$m_c = 1.4$	$m_u = 0.25$	$m_s = 0.37$
	$m_e = 0.000511$	$m_\mu = 0.106$	$m_\tau = 1.78$	$m_{B_s} = 5.367$
	$m_B = 5.279$	$m_{D_0^*} = 2.343$	$m_{D_{s0}^*} = 2.317$	$m_{D_{s1}} = 2.460$
	$m_{D'_{s1}} = 2.536$	$m_{D_1} = 2.422$	$m_{D'_1} = 2.412$	
CKM	$V_{cb} = (40.8 \pm 1.4) \times 10^{-3}$			
shape parameters(GeV)	$\beta'_B = 0.555^{+0.048}_{-0.048}$	$\beta'_{B_s} = 0.628^{+0.035}_{-0.034}$	$\beta'_{D_0^*} = 0.373^{+0.063}_{-0.059}$	
	$\beta'_{D_{s0}^*} = 0.325^{+0.043}_{-0.043}$	$\beta'_{D_{s1}} = 0.342^{+0.030}_{-0.034}$	$\beta'_{D'_{s1}} = 0.342^{+0.039}_{-0.039}$	
	$\beta'_{D_1} = 0.332^{+0.031}_{-0.034}$	$\beta'_{D'_1} = 0.329^{+0.038}_{-0.040}$		
Lifetimes(s)	$\tau_{B_s} = (1.520 \pm 0.005) \times 10^{-12}$		$\tau_{B^\pm} = (1.638 \pm 0.004) \times 10^{-12}$	
	$\tau_{B^0} = (1.519 \pm 0.004) \times 10^{-12}$			

The adopted input parameters [47], such as the constituent quark masses, the hadron and lepton masses, the B meson lifetime and the Cabibbo-Kobayashi-Maskawa (CKM) matrix element V_{cb} , in our numerical calculations are listed in Table I. In the calculations

of the helicity amplitudes, the transition form factors are the most important inputs, some of which have been calculated in our previous work [44]. The parameterized form factors are extrapolated from the space-like region to the time-like region by using following expression,

$$F(q^2) = \frac{F(0)}{1 - aq^2/m^2 + bq^4/m^4}, \quad (40)$$

where m represents the initial meson mass and $F(q^2)$ denotes the different form factors. The values of a and b can be obtained by performing a 3-parameter fit to the form factors in the range $-15\text{GeV}^2 \leq q^2 \leq 0$, which are collected in Table II. The uncertainties arise from the decay constants of the initial $B_{(s)}$ meson and the final state mesons. Certainly, in order to compare with the results given in other works, we also give the form factors of the transitions $B_{(s)} \rightarrow D_{(s)1}^{3/2}, D_{(s)1}^{1/2}$ under the heavy quark limit, which are shown in Table III. Obviously, our results are consistent with the previous CLFQM [43] and ISGW2 [63] calculations. The signs of the form factors of the transitions $B_{(s)} \rightarrow D_{(s)1}^{1/2}$ between ours and the other two theoretical predictions [43, 63] are opposite because the definitions for the $D_{(s)1}^{1/2}$ mixing formula shown in Eq. (2) are different.

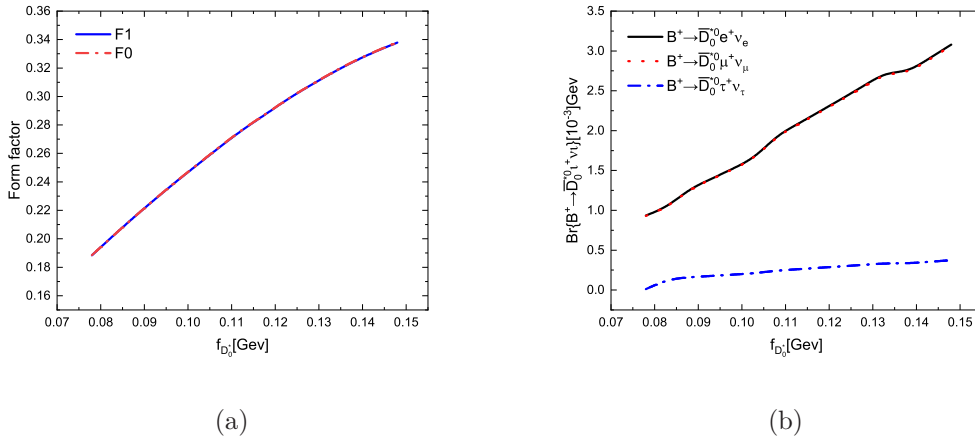


FIG. 2: The dependencies of the form factors of the transition $B \rightarrow D_0^*$ (left) and the branching ratios of the semileptonic decays $B \rightarrow D_0^* \ell \nu_\ell$ (right) on the decay constant $f_{D_0^*}$.

TABLE II: The form factors of the transtions $B_{(s)} \rightarrow D_0^*, D_{s0}^*, D_{s1}, D'_{s1}, D_1$ and D'_1 in the CLFQM. The uncertainties are from the decay constants of $B_{(s)}$ and the final state mesons.

	$F_i(q^2 = 0)$	$F_i(q_{max}^2)$	a	b
$F_1^{BD_0^*}$	$0.25^{+0.03+0.05}_{-0.02-0.05}$	$0.30^{+0.03+0.06}_{-0.03-0.07}$	$0.70^{+0.04+0.03}_{-0.05-0.11}$	$0.65^{+0.08+0.03}_{-0.07-0.07}$
$F_0^{BD_0^*}$	$0.25^{+0.03+0.05}_{-0.02-0.05}$	$0.22^{+0.02+0.04}_{-0.01-0.04}$	$-0.38^{+0.04+0.05}_{-0.04-0.02}$	$0.21^{+0.07+0.08}_{-0.07-0.08}$
$F_1^{B_s D_{s0}^*}$	$0.21^{+0.02+0.04}_{-0.01-0.04}$	$0.24^{+0.02+0.05}_{-0.01-0.05}$	$0.63^{+0.05+0.07}_{-0.06-0.12}$	$0.78^{+0.08+0.01}_{-0.09-0.04}$
$F_0^{B_s D_{s0}^*}$	$0.21^{+0.02+0.04}_{-0.01-0.04}$	$0.18^{+0.02+0.03}_{-0.01-0.03}$	$-0.43^{+0.01+0.01}_{-0.00-0.02}$	$0.28^{+0.03+0.01}_{-0.06-0.04}$
$A^{B_s D_{s1}}$	$0.20^{+0.01+0.02}_{-0.01-0.02}$	$0.18^{+0.02+0.03}_{-0.01-0.02}$	$-0.27^{+0.06+0.8}_{-0.07-0.09}$	$0.11^{+0.02+0.02}_{-0.02-0.03}$
$V_0^{B_s D_{s1}}$	$0.40^{+0.02+0.04}_{-0.02-0.04}$	$0.42^{+0.02+0.05}_{-0.02-0.05}$	$-0.17^{+0.02+0.04}_{-0.04-0.06}$	$-0.02^{+0.01+0.00}_{-0.00-0.01}$
$V_1^{B_s D_{s1}}$	$0.58^{+0.01+0.03}_{-0.02-0.04}$	$0.57^{+0.01+0.03}_{-0.02-0.04}$	$-0.05^{+0.01+0.01}_{-0.01-0.01}$	$0.02^{+0.00+0.01}_{-0.00-0.00}$
$V_2^{B_s D_{s1}}$	$-0.05^{+0.01+0.02}_{-0.00-0.01}$	$-0.05^{+0.01+0.03}_{-0.00-0.02}$	$0.56^{+0.06+0.22}_{-0.06-0.25}$	$2.50^{+0.25+1.67}_{-0.20-1.30}$
$A^{B_s D'_{s1}}$	$0.08^{+0.01+0.02}_{-0.01-0.02}$	$0.03^{+0.01+0.01}_{-0.02-0.03}$	$2.05^{+0.13+0.35}_{-0.10-0.35}$	$5.57^{+0.25+0.50}_{-0.20-0.41}$
$V_0^{B_s D'_{s1}}$	$-0.08^{+0.01+0.04}_{-0.01-0.04}$	$-0.05^{+0.02+0.05}_{-0.01-0.04}$	$1.24^{+0.05+0.23}_{-0.06-0.25}$	$0.74^{+0.02+0.21}_{-0.02-0.17}$
$V_1^{B_s D'_{s1}}$	$0.17^{+0.02+0.04}_{-0.03-0.03}$	$0.15^{+0.01+0.02}_{-0.03-0.03}$	$-0.52^{+0.06+0.06}_{-0.05-0.06}$	$0.36^{+0.01+0.03}_{-0.00-0.08}$
$V_2^{B_s D'_{s1}}$	$0.11^{+0.01+0.01}_{-0.02-0.02}$	$0.10^{+0.01+0.01}_{-0.02-0.02}$	$0.25^{+0.06+0.06}_{-0.07-0.07}$	$-0.07^{+0.03+0.01}_{-0.04-0.03}$
A^{BD_1}	$0.21^{+0.02+0.02}_{-0.01-0.01}$	$0.20^{+0.02+0.02}_{-0.02-0.02}$	$-0.23^{+0.10+0.09}_{-0.09-0.09}$	$0.09^{+0.02+0.02}_{-0.02-0.02}$
$V_0^{BD_1}$	$0.42^{+0.03+0.04}_{-0.02-0.04}$	$0.44^{+0.04+0.05}_{-0.02-0.05}$	$0.16^{+0.02+0.03}_{-0.02-0.05}$	$-0.02^{+0.00+0.01}_{-0.00-0.01}$
$V_1^{BD_1}$	$0.57^{+0.03+0.03}_{-0.01-0.04}$	$0.56^{+0.03+0.03}_{-0.02-0.04}$	$-0.07^{+0.00+0.01}_{-0.01-0.00}$	$0.02^{+0.00+0.00}_{-0.00-0.00}$
$V_2^{BD_1}$	$-0.06^{+0.01+0.02}_{-0.01-0.02}$	$-0.06^{+0.01+0.04}_{-0.01-0.03}$	$0.57^{+0.06+0.17}_{-0.07-0.20}$	$2.13^{+0.21+1.30}_{-0.18-1.17}$
$A^{BD'_1}$	$0.07^{+0.02+0.02}_{-0.02-0.02}$	$0.02^{+0.03+0.01}_{-0.02-0.02}$	$-1.90^{+0.09+0.12}_{-0.10-0.14}$	$5.64^{+0.22+1.59}_{-0.18-1.29}$
$V_0^{BD'_1}$	$-0.08^{+0.02+0.04}_{-0.02-0.03}$	$-0.06^{+0.02+0.06}_{-0.02-0.03}$	$-0.11^{+0.01+0.06}_{-0.04-0.11}$	$3.67^{+0.05+0.51}_{-0.05-0.51}$
$V_1^{BD'_1}$	$0.14^{+0.04+0.03}_{-0.04-0.03}$	$0.13^{+0.03+0.03}_{-0.04-0.02}$	$-0.36^{+0.04+0.04}_{-0.06-0.06}$	$0.09^{+0.01+0.01}_{-0.01-0.01}$
$V_2^{BD'_1}$	$0.10^{+0.03+0.02}_{-0.02-0.02}$	$0.11^{+0.03+0.02}_{-0.04-0.04}$	$0.19^{+0.06+0.06}_{-0.09-0.09}$	$0.00^{+0.01+0.01}_{-0.00-0.01}$

The branching ratios of the decays $B_{(s)} \rightarrow D_{(s)0}^* \ell \nu_\ell$ are shown in Table IV. For comparison, the values given by other theoretical approaches and the current experiments are also listed. One can find that the branching ratios of the decays $B^+ \rightarrow \bar{D}_0^{*0} \ell^+ \nu_\ell$ are larger than the results from the QCD sum rules (QCDSRs) [32] and the heavy quark effective field theory (HQEFT) [51]. Obviously, our predictions are consistent with the previous CLFQM calculations [52] and the differences are mainly due to the different values of the decay constant $f_{D_0^*}$. In Figure 2, the changing trends of the form factors $F_1^{BD_0^*}(q^2 = 0)(F_0^{BD_0^*}(q^2 = 0))$ and the branching ratios of the decays $B^+ \rightarrow \bar{D}_0^{*0} \ell^+ \nu_\ell$ with $f_{D_0^*}$ are plotted, respectively. Both of them increase with $f_{D_0^*}$. The branching ratios of the decays $B^0 \rightarrow D_0^{*-} \ell^+ \nu_\ell$ can agree with QCD LCSRs under scenario 2 (S2), where the broad resonance D_0^* was considered as consisting of the two resonances $D_0^*(2105)$ and $D_0^*(2451)$

[53]. While it seems to be too large in scenario 1 (S1), where D_0^* was considered as a single resonance [53]. Certainly, there still exist large errors in both S1 and S2. Our predictions are much smaller than those given in the LCSRs approach [54], where a very large form factor $F_0^{BD_0^*}(q^2 = 0) = 0.94$ was used in the calculations. There exists a similar situation for the decays $B_s^0 \rightarrow D_{s0}^{*-} \ell^+ \nu_\ell$. It is surprising that a large value $(2.2 \pm 0.86) \times 10^{-2}$ was measured by Belle [55] in 2008, latter a more large one $(4.4 \pm 1.0) \times 10^{-2}$ was given by BaBar [57], while Belle updated their measurement with only a small upper limit $< 0.44 \times 10^{-3}$ obtained. In theory, the branching ratios of the decays $B^+ \rightarrow \bar{D}_0^{*0} \ell'^+ \nu_{\ell'}$ and $B^0 \rightarrow D_0^{*-} \ell'^+ \nu_{\ell'}$ should be not much difference. In order to clarifying this puzzle, we urge our experimental colleagues to perform further more precise measurements. In Ref. [58], the authors calculated the branching ratios based on the general HQET expansion, the so called the Leibovich-Ligeti-Stewart-Wise (LLSW) scheme, combining other theoretical results and the constrains from experimental measurements, which are smaller than nearly all the present available predictions.

TABLE III: Form factors of the transitions $B_{(s)} \rightarrow D_{s1}^{3/2}, D_{s1}^{1/2}, D_1^{3/2}$ and $D_1^{1/2}$ at $q^2 = 0$ together with other theoretical results.

Transitions	References	$A(0)$	$V_0(0)$	$V_1(0)$	$V_2(0)$
$B_s \rightarrow D_{s1}^{3/2}$	This work	0.19	0.41	0.55	-0.07
	CLFQM ^a [63]	0.24	0.49	0.57	-0.09
$B_s \rightarrow D_{s1}^{1/2}$	This work	0.10	-0.03	0.24	0.11
	CLFQM ^a [63]	-0.17	0.13	-0.25	-0.17
$B \rightarrow D_1^{3/2}$	This work	0.20	0.43	0.55	-0.07
	CLFQM [43]	0.23	0.47	0.55	-0.09
	ISGW2 [43]	0.16	0.43	0.40	-0.12
	CLFQM [63]	0.25	0.52	0.58	-0.10
$B \rightarrow D_1^{1/2}$	This work	0.09	-0.02	0.21	0.09
	CLFQM ^a [43]	-0.12	0.08	-0.19	-0.12
	ISGW2 ^a [43]	-0.16	0.18	-0.19	-0.18
	CLFQM ^a [63]	-0.13	0.11	-0.19	-0.14

^a Due to the signs of the $D_{(s)1}^{1/2}$ mixing formula Eq. (2) between this work and Refs. [43, 63] are opposite, the corresponding results are just contrary with our predictions.

TABLE IV: Branching ratios (10^{-3}) of the semileptonic decays $B_{(s)} \rightarrow D_{(s)0}^* \ell \nu_\ell$.

References	$B^+ \rightarrow \bar{D}_0^{*0} e^+ \nu_e$	$B^+ \rightarrow \bar{D}_0^{*0} \mu^+ \nu_\mu$	$B^+ \rightarrow \bar{D}_0^{*0} \tau^+ \nu_\tau$
This work	$1.66_{-0.27-0.62}^{+0.43+0.74}$	$1.65_{-0.26-0.62}^{+0.43+0.74}$	$0.21_{-0.03-0.08}^{+0.06+0.10}$
QCDSRs [32]	$0.61_{-0.21-0.05}^{+0.28+0.04}$	$0.61_{-0.21-0.05}^{+0.28+0.04}$	$0.04_{-0.01-0.00}^{+0.02+0.00}$
CLFQM [52]	2.31 ± 0.25	2.31 ± 0.25	0.30 ± 0.03
HQEFT [51]	0.50 ± 0.16	0.50 ± 0.16	–
PDG [47]	1.35 ± 0.75	1.35 ± 0.75	–
References	$B^0 \rightarrow D_0^{*-} e^+ \nu_e$	$B^0 \rightarrow D_0^{*-} \mu^+ \nu_\mu$	$B^0 \rightarrow D_0^{*-} \tau^+ \nu_\tau$
This work	$1.54_{-0.25-0.57}^{+0.40+0.69}$	$1.53_{-0.25-0.57}^{+0.40+0.69}$	$0.19_{-0.03-0.07}^{+0.05+0.09}$
QCD LCSRs [53] ^a	$3.6_{-3.0}^{+5.1}$	$3.6_{-3.0}^{+5.1}$	$0.39_{-0.31}^{+0.51}$
QCD LCSRs [53] ^b	$1.6_{-1.4}^{+3.2}$	$1.6_{-1.4}^{+3.2}$	$0.24_{-0.21}^{+0.47}$
LCSRs [54]	$8.7_{-2.8}^{+5.1}$	$8.7_{-2.8}^{+5.1}$	$1.1_{-0.3}^{+0.6}$
LLSW [58]	0.51 ± 0.12	0.51 ± 0.12	0.050 ± 0.013
BaBar [57]	4.4 ± 1.0	4.4 ± 1.0	–
Belle [55]	2.0 ± 0.86	2.0 ± 0.86	–
Belle [56]	< 0.44	< 0.44	–
References	$B_s^0 \rightarrow D_{s0}^{*-} e^+ \nu_e$	$B_s^0 \rightarrow D_{s0}^{*-} \mu^+ \nu_\mu$	$B_s^0 \rightarrow D_{s0}^{*-} \tau^+ \nu_\tau$
This work	$1.26_{-0.13-0.45}^{+0.26+0.55}$	$1.25_{-0.13-0.45}^{+0.26+0.55}$	$0.18_{-0.02-0.07}^{+0.04+0.08}$
QCDSRs [32]	$0.72_{-0.26-0.06}^{+0.30+0.04}$	$0.71_{-0.25-0.05}^{+0.33+0.04}$	$0.06_{-0.02-0.00}^{+0.03+0.00}$
CUM [59]	1.3	1.3	–
QCD LCSRs [53]	$1.9_{-1.7}^{+3.8}$	$1.9_{-1.7}^{+3.8}$	$0.26_{-0.22}^{+0.49}$
QCDSRs [64]	$0.9 \sim 2.0$	$0.9 \sim 2.0$	–
QCDSRs [65]	1.0	1.0	0.1
LCSRs [50]	$2.3_{-1.0}^{+1.2}$	$2.3_{-1.0}^{+1.2}$	$0.57_{-0.23}^{+0.28}$
CQM [60]	$4.90 \sim 5.71$	$4.9 \sim 5.71$	–
RQM [62]	3.6 ± 0.4	3.6 ± 0.4	0.19 ± 0.02
LSCRs [54]	6.0 ± 1.9	6.0 ± 1.9	$0.82_{-0.20}^{+0.18}$

^a Results obtained in scenario 1 (S1), where D_0^* was considered as a single broad resonance with mass being (2343 ± 10) MeV and width (229 ± 16) MeV.

^b Results obtained in scenario 2 (S2), where D_0^* was assumed to consist of two scalar resonances $D_0^*(2105)$ and $D_0^*(2451)$.

Then we compare our predictions for the branching ratios of the decays $B_s^0 \rightarrow D_{s0}^{*-} \ell^+ \nu_\ell$ with the results obtained from other approaches. One can find that our results are consistent with those given in the chiral unitary approach (CUA) [59], the QCDSRs [32], the QCD LCSRs [53] and the LCSRs [50] within errors. While they are much smaller than the constituent quark meson (CQM) [60] and the LCSRs [54] calculations. Although the LCSRs was used in both Ref. [50] and Ref. [54], their results are very different. It is because of the different correlation function, which is taken between the vacuum and $D_{s0}^*(B)$ with the $B(D_{s0}^*)$ meson being interpolated by a local current for the former (the latter).

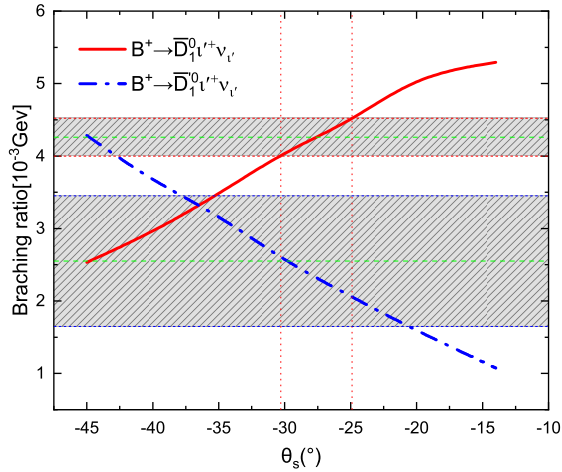
The form factor of the transition $B_s \rightarrow D_{s0}^*$ obtained in the latter (the so called B-meson LCSRs) is about 0.80, which is larger than 0.53 calculated by the former (the so called the conventional light meson LCSRs). Further experimental and theoretical researches are needed to clarify these divergences and puzzles.

TABLE V: Branching ratios (10^{-3}) of the semileptonic decays $B \rightarrow D_1^{(\prime)\ell}\nu_\ell$ and $B_s \rightarrow D_{s1}^{(\prime)\ell}\nu_\ell$.

References	$B^+ \rightarrow \bar{D}_1^0 e^+ \nu_e$	$B^+ \rightarrow \bar{D}_1^0 \mu^+ \nu_\mu$	$B^+ \rightarrow \bar{D}_1^0 \tau^+ \nu_\tau$
This work	$6.21_{-0.67-0.28-0.90}^{+0.94+0.43+1.00}$	$6.16_{-0.66-0.27-0.89}^{+0.93+0.42+0.99}$	$0.57_{-0.05-0.04-0.07}^{+0.08+0.03+0.07}$
QCDSRs [32]	$7.26_{-2.87-0.49}^{+3.60+0.51}$	$7.19_{-2.84-0.48}^{+3.56+0.50}$	$0.46_{-0.17-0.03}^{+0.22+0.03}$
LLSW [58]	6.40 ± 0.44	6.40 ± 0.44	0.63 ± 0.06
HQEFT [66]	5.9 ± 1.6	5.9 ± 1.6	–
PDG [47]	4.26 ± 0.26	4.26 ± 0.26	–
References	$B^+ \rightarrow \bar{D}_1^{\prime 0} e^+ \nu_e$	$B^+ \rightarrow \bar{D}_1^{\prime 0} \mu^+ \nu_\mu$	$B^+ \rightarrow \bar{D}_1^{\prime 0} \tau^+ \nu_\tau$
This work	$0.15_{-0.09-0.03-0.06}^{+0.15+0.07+0.08}$	$0.15_{-0.09-0.03-0.06}^{+0.15+0.07+0.08}$	$0.02_{-0.01-0.02-0.00}^{+0.01+0.00+0.00}$
QCDSRs [32]	$0.68_{-0.24-0.05}^{+0.31+0.04}$	$0.67_{-0.23-0.05}^{+0.31+0.04}$	$0.05_{-0.02-0.00}^{+0.05+0.00}$
LLSW [58]	0.46 ± 0.37	0.46 ± 0.37	0.03 ± 0.03
HQEFT [51]	0.48 ± 0.16	0.48 ± 0.16	–
PDG [47]	2.55 ± 0.90	2.55 ± 0.90	–
References	$B_s^0 \rightarrow D_{s1}^- e^+ \nu_e$	$B_s^0 \rightarrow D_{s1}^- \mu^+ \nu_\mu$	$B_s^0 \rightarrow D_{s1}^- \tau^+ \nu_\tau$
This work	$6.17_{-0.91-0.62-0.52}^{+0.94+0.21+0.42}$	$6.13_{-0.94-0.61-0.52}^{+0.91+0.21+0.42}$	$0.62_{-0.05-0.06-0.00}^{+0.03+0.04+0.00}$
QCDSRs [32]	$6.31_{-2.44-0.43}^{+3.07+0.44}$	$6.25_{-2.42-0.42}^{+3.03+0.44}$	$0.38_{-0.14-0.03}^{+0.18+0.03}$
CQM [60]	$7.52 \sim 8.69$	$7.52 \sim 8.69$	–
QCDSRs [61]	4.90	4.90	–
RQM [62]	8.40 ± 0.90	8.40 ± 0.90	0.49 ± 0.05
References	$B_s^0 \rightarrow D_{s1}^{\prime -} e^+ \nu_e$	$B_s^0 \rightarrow D_{s1}^{\prime -} \mu^+ \nu_\mu$	$B_s^0 \rightarrow D_{s1}^{\prime -} \tau^+ \nu_\tau$
This work	$0.18_{-0.07-0.07-0.09}^{+0.06+0.07+0.07}$	$0.18_{-0.07-0.07-0.09}^{+0.06+0.07+0.07}$	$0.02_{-0.00-0.01-0.00}^{+0.01+0.01+0.00}$
QCDSRs [32]	$0.65_{-0.23-0.05}^{+0.30+0.04}$	$0.64_{-0.23-0.05}^{+0.30+0.04}$	$0.05_{-0.02-0.00}^{+0.03+0.00}$
RQM [62]	1.90 ± 0.02	1.90 ± 0.02	0.15 ± 0.02

We calculate the branching ratios of the decays $B_s^0 \rightarrow D_{s1}^{(\prime)\ell^+}\nu_\ell$ and $B^+ \rightarrow \bar{D}_1^{(\prime)\ell^+}\nu_\ell$, which are listed in Table V with other theoretical predictions and data for comparison. All the theoretical predictions show that the branching ratios of the decays $B_s^0 \rightarrow D_{s1}^-\ell^+\nu_\ell$ are (much) larger than those of the decays $B_s^0 \rightarrow D_{s1}^{\prime -}\ell^+\nu_\ell$. This is because that the related form factors of the transition $B_s \rightarrow D_{s1}$ are much larger than those of the transition $B_s \rightarrow D_{s1}^{\prime}$. There exists a similar situation between the decays $B^+ \rightarrow \bar{D}_1^0\ell^+\nu_\ell$ and $B^+ \rightarrow \bar{D}_1^{\prime 0}\ell^+\nu_\ell$. One can find that the branching ratios of the decays $B_{(s)} \rightarrow D_{(s)1}\ell\nu_\ell$ are comparable with the results given by most theoretical calculations, such as the QCDSRs [32, 61], the CQM [60], the relativistic quark model (RQM) [62], the LLSW [58], the HQEFT [51], and so on. Certainly, they are also consistent well with the present available data [47]. While for the decays $B^+ \rightarrow \bar{D}_1^{\prime 0}\ell^+\nu_\ell$, their branching ratios given by all the

theoretical predictions are smaller than the data measured by Belle [11]. Therefore we urge our experimental colleagues to accurately measure these decays. It is very helpful to probe the inner structures of the resonant states $D_{(s)1}$ and $D'_{(s)1}$ by clarifying the tension between theory and experiment, which is the so called 1/2 vs 3/2 puzzle. In order to explain this puzzle, we calculate the dependences of the branching ratios of the decays $B \rightarrow D_1^{(\prime)} \ell' \nu_{\ell'}$ on the mixing angle θ_s , which are shown in Figure 3, where the branching ratios for the decays $B^+ \rightarrow D_1^{(\prime)0} \ell' \nu_{\ell'}$ increase (decrease) with the mixing angle θ_s . The upper (lower) shadow band and its horizontal image center line refers to the experimentally achievable range and the center value for the branching ratios of the decays $B^+ \rightarrow D_1^0 \ell' \nu_{\ell'}$ ($B^+ \rightarrow \bar{D}_1^0 \ell' \nu_{\ell'}$), respectively. One can find that taking some negative mixing angle θ_s values within a range from -30.3° to -24.9° can explain the data, which correspond to θ within the range $5^\circ \sim 10.4^\circ$. It is similar for the decays $B_s^0 \rightarrow D_{s1}^{(\prime)-} \ell^+ \nu_{\ell'}$ and $B^+ \rightarrow \bar{D}_1^{(\prime)0} \tau^+ \nu_{\tau}$, $B_s^0 \rightarrow D_{s1}^{(\prime)-} \tau^+ \nu_{\tau}$, the dependencies of their branching ratios on the mixing angle θ_s are shown in Figure 4. All of these decays shown that the branching ratios of the decays with $D_{(s)1}$ involved increase with the mixing angle θ_s , while it is contrary for those of the decays with $D'_{(s)1}$ involved.



(a)

FIG. 3: The mixing angle θ_s dependencies of the branching ratios for the semileptonic decays $B^+ \rightarrow \bar{D}_1^0 \ell^+ \nu_{\ell'}$ (the red solid line) and $B^+ \rightarrow \bar{D}_1^0 \ell^+ \nu_{\ell'}$ (the blue dash-dotted line). The upper (lower) shadow band and its horizontal image center line refers to the experimentally achievable range and the center value for the branching ratios of the decays $B^+ \rightarrow D_1^0 \ell' \nu_{\ell'}$ ($B^+ \rightarrow \bar{D}_1^0 \ell' \nu_{\ell'}$), respectively.

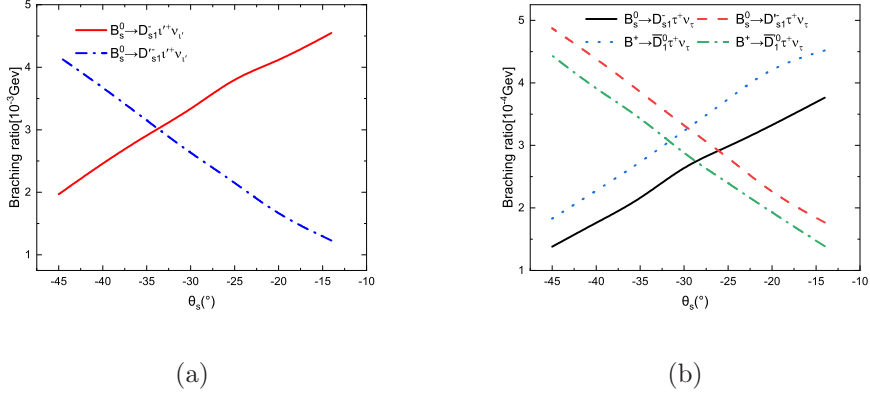


FIG. 4: The mixing angle θ_s dependencies of the branching ratios for the semileptonic decays $B_s^0 \rightarrow D_{s1}^{(l)-} \ell^+ \nu_\ell$ (a) and $B^+ \rightarrow \bar{D}_1^{(l)0} \tau^+ \nu_\tau, B_s^0 \rightarrow D_{s1}^{(l)-} \tau^+ \nu_\tau$ (b).

In Table VI, we also calculate the lepton flavor universality ratios, which are defined as

$$R(D_{(s)}^{**}) = \frac{\Gamma(B \rightarrow D_{(s)}^{**} \tau \nu_\tau)}{\Gamma(B \rightarrow D_{(s)}^{**} \ell' \nu_{\ell'})}, \quad (41)$$

where a large part of the theoretical and experimental uncertainties, especially the errors from the form factors, can be canceled. One can find that most of our predictions are comparable with other theoretical results. Compared to the S1 and S2 values given in the QCD LCSRs [53], our prediction for $R(D_0^*)$ gives a moderate value.

A. Physical observables

In our study of semileptonic decays, we define two additional physical observables, namely the longitudinal polarization fraction f_L and the forward-backward asymmetry A_{FB} , to account for the impact of lepton mass and provide a more detailed physical picture. The results of these two physical observables are listed in Tables VII and VIII, respectively. In Table VII, we can clearly find that the longitudinal polarization fractions f_L between the decays $B_{(s)} \rightarrow D_{(s)1}^{(l)} e^+ \nu_e$ and $B_{(s)} \rightarrow D_{(s)1}^{(l)} \mu^+ \nu_\mu$ are very close to each other, which reflect the lepton flavor universality (LFU). In order to investigate the dependences of the polarizations on the different q^2 , we divide the full energy region into two segments for each decay and calculate the longitudinal polarization fractions accordingly. Region 1 is defined as $m_\ell^2 < q^2 < \frac{(m_{B(s)} - m_{D(s)1}^{(l)})^2 + m_\ell^2}{2}$ and Region 2 is $\frac{(m_{B(s)} - m_{D(s)1}^{(l)})^2 + m_\ell^2}{2} < q^2 <$

$(m_{B_{(s)}} - m_{D_{(s)1}^{(\prime)}})^2$. Obviously, the longitudinal polarization fraction in Region 1 is larger than that in Region 2 for each decay. Furthermore, for the decays with $D_{(s)1}$ involved in the final states the longitudinal polarization is dominant, while it is contrary for the decays with $D'_{(s)1}$ involved. These results can be validated by the future high-luminosity experiments.

TABLE VI: The lepton flavor universality ratios of the transitions $B_{(s)} \rightarrow D_0^*, D_{s0}^*, D_{s1}^{(\prime)}, D_1^{(\prime)}$.

Decays	Ratios	Predicted values	Decays	Ratios	Predicted values
$B^+ \rightarrow \bar{D}_0^{*0} \ell^+ \nu_\ell$	$R(\bar{D}_0^*)$	$0.127^{+0.003+0.003}_{-0.001-0.000}$	$B_s^0 \rightarrow D_{s1}^- \ell^+ \nu_\ell$	$R(D_{s1})$	$0.102^{+0.007+0.003}_{-0.009-0.001}$
		$0.063^{+0.001}_{-0.002}$ [32]			0.061 ± 0.003 [32]
		0.08 ± 0.03 [35]			0.09 ± 0.02 [36]
$B^0 \rightarrow D_0^{*-} \ell^+ \nu_\ell$	$R(D_0^*)$	$0.127^{+0.001+0.002}_{-0.001-0.002}$	$B_s^0 \rightarrow D_{s1}'^- \ell^+ \nu_\ell$	$R(D_{s1}')$	$0.111^{+0.014+0.009}_{-0.029-0.020}$
		0.099 ± 0.015 [58]			$0.084^{+0.001}_{-0.002}$ [32]
		$0.11^{+0.03}_{-0.01}(S1), 0.16^{+0.04}_{-0.02}(S2)^1$ [53]			0.07 ± 0.03 [36]
$B_s^0 \rightarrow D_{s0}^{*0} \ell^+ \nu_\ell$	$R(D_{s0}^*)$	$0.147^{+0.003+0.001}_{-0.004-0.003}$	$B^+ \rightarrow \bar{D}_1^0 \ell^+ \nu_\ell$	$R(D_1)$	$0.091^{+0.001+0.003}_{-0.002-0.004}$
		$0.080^{+0.001}_{-0.002}$ [32]			$0.064^{+0.003}_{-0.003}$ [32]
		0.09 ± 0.04 [36]			0.10 ± 0.02 [35]
		$0.14^{+0.07}_{-0.02}$ [53]			0.098 ± 0.007 [58]
			$B^+ \rightarrow \bar{D}_1^{\prime 0} \ell^+ \nu_\ell$	$R(D_1')$	$0.110^{+0.030+0.051}_{-0.010-0.025}$
					$0.076^{+0.001}_{-0.002}$ [32]
					0.05 ± 0.02 [35]
					0.074 ± 0.012 [58]

¹ The definitions of S1 and S2 are given in Table IV.

TABLE VII: The longitudinal polarization fractions f_L for the decays $B_s \rightarrow D_{s1}^{(\prime)-} \ell^+ \nu_\ell$ and $B^+ \rightarrow \bar{D}_1^{(\prime)0} \ell^+ \nu_\ell$ in Region 1 and Region 2.

Observables	Region 1	Region 2	Total	Observables	Region 1	Region 2	Total
$f_L(B_s^0 \rightarrow D_{s1}^- e^+ \nu_e)$	0.81	0.50	0.71	$f_L(B_s^0 \rightarrow D_{s1}'^- e^+ \nu_e)$	0.42	0.12	0.31
$f_L(B_s^0 \rightarrow D_{s1}^- \mu^+ \nu_\mu)$	0.81	0.50	0.71	$f_L(B_s^0 \rightarrow D_{s1}'^- \mu^+ \nu_\mu)$	0.42	0.12	0.31
$f_L(B_s^0 \rightarrow D_{s1}^- \tau^+ \nu_\tau)$	0.66	0.48	0.56	$f_L(B_s^0 \rightarrow D_{s1}'^- \tau^+ \nu_\tau)$	0.23	0.24	0.24
$f_L(B^+ \rightarrow \bar{D}_1^0 e^+ \nu_e)$	0.81	0.50	0.72	$f_L(B^+ \rightarrow \bar{D}_1^{\prime 0} e^+ \nu_e)$	0.54	0.11	0.39
$f_L(B^+ \rightarrow \bar{D}_1^0 \mu^+ \nu_\mu)$	0.81	0.50	0.72	$f_L(B^+ \rightarrow \bar{D}_1^{\prime 0} \mu^+ \nu_\mu)$	0.54	0.11	0.39
$f_L(B^+ \rightarrow \bar{D}_1^0 \tau^+ \nu_\tau)$	0.67	0.49	0.56	$f_L(B^+ \rightarrow \bar{D}_1^{\prime 0} \tau^+ \nu_\tau)$	0.32	0.25	0.28

In Figure 5, we plot the q^2 dependencies of the differential decay rates for the channels $B_{(s)} \rightarrow D_{(s)0}^* \ell \nu_\ell$ and $B_{(s)} \rightarrow D_{(s)1}^{(\prime)} \ell \nu_\ell$. One can find that the line shapes of these differential distributions are constrained by the phase space, in other words, the lepton mass. The polarization needs to be considered in the decays $B_s \rightarrow D_{s1}^{(\prime)} \ell \nu_\ell$ and $B \rightarrow D_1^{(\prime)} \ell \nu_\ell$, which is shown in Figures 5(c)-5(h). It is obvious that for the decays with $D_{(s)1}$ involved the longitudinal polarization is dominant in small q^2 region and comparable with the transverse ones in large q^2 region. While for the decays with $D'_{(s)1}$ involved the transverse polarizations are dominant, especially in large q^2 region. It is interesting that taking some special q^2 values for the decays $B \rightarrow D'_1 \ell \nu_\ell$ and $B_s \rightarrow D'_{s1} \ell \nu_\ell$, we can find that the contribution from the longitudinal polarization almost disappears with only the transverse polarizations left, which is shown in Figures 5(d) and 5(f). Maybe such a phenomenon can be checked in the future LHC and Super KEKB experiments to test the present mixing mechanism.

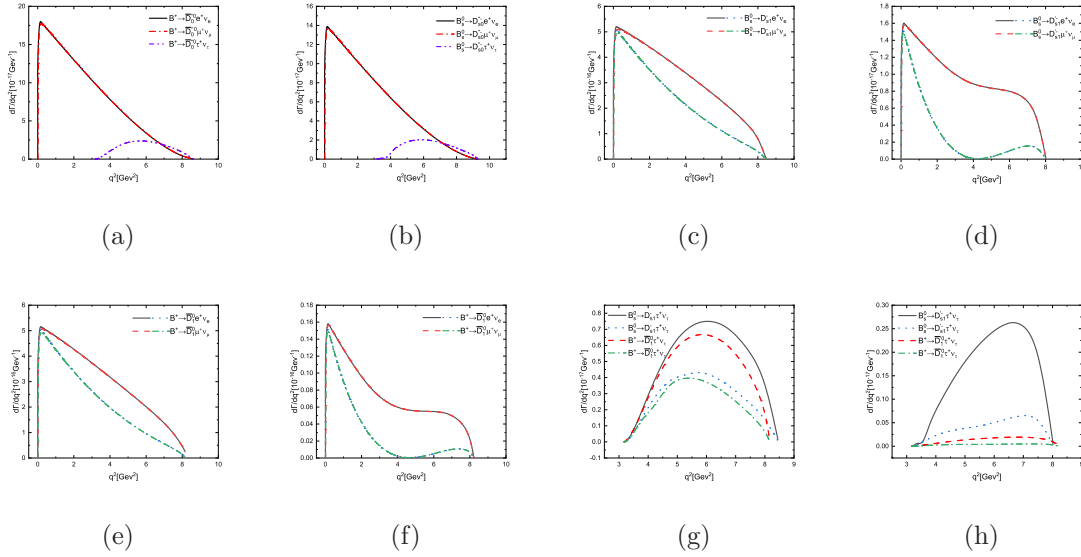


FIG. 5: The q^2 dependencies of differential decay rates $d\Gamma/dq^2$ and $d\Gamma^L/dq^2$ for the decays $B_{(s)} \rightarrow D_{(s)0}^* \ell \nu_\ell$ and $B_{(s)} \rightarrow D_{(s)1}^{(\prime)} \ell \nu_\ell$.

TABLE VIII: The forward-backward asymmetries A_{FB} for the decays $B_{(s)} \rightarrow D_{(s)0}^* \ell \nu \ell$ and $B_{(s)} \rightarrow D_{(s)1}^{(\prime)} \ell \nu \ell$.

Channels		$B^+ \rightarrow \bar{D}_0^* e^+ \nu_e$	$B^+ \rightarrow \bar{D}_0^* \mu^+ \nu_\mu$	$B^+ \rightarrow \bar{D}_0^* \tau^+ \nu_\tau$
A_{FB}	This work	$(5.820^{+1.494+2.582}_{-0.904-2.108}) \times 10^{-7}$	$0.020^{+0.005+0.009}_{-0.003-0.007}$	$0.383^{+0.102+0.177}_{-0.063-0.143}$
Channels		$B_s^0 \rightarrow D_{s0}^{*-} e^+ \nu_e$	$B_s^0 \rightarrow D_{s0}^{*-} \mu^+ \nu_\mu$	$B_s^0 \rightarrow D_{s0}^{*-} \tau^+ \nu_\tau$
A_{FB}	This work [67]	$(5.465^{+1.100+2.298}_{-0.515-1.898}) \times 10^{-7}$ 8.22×10^{-7}	$0.019^{+0.004+0.010}_{-0.002-0.007}$ 0.016	$0.381^{+0.079+0.168}_{-0.038-0.138}$ 0.39
Channel		$B_s^0 \rightarrow D_{s1}^- e^+ \nu_e$	$B_s^0 \rightarrow D_{s1}^- \mu^+ \nu_\mu$	$B_s^0 \rightarrow D_{s1}^- \tau^+ \nu_\tau$
A_{FB}	This work [67]	$-0.175^{+0.016+0.027+0.011}_{-0.014-0.016-0.017}$ -0.19	$-0.174^{+0.016+0.026+0.010}_{-0.014-0.017-0.017}$ -0.18	$-0.129^{+0.010+0.021+0.003}_{-0.015-0.017-0.016}$ 0.10
Channels		$B_s^0 \rightarrow D_{s1}^{\prime-} e^+ \nu_e$	$B_s^0 \rightarrow D_{s1}^{\prime-} \mu^+ \nu_\mu$	$B_s^0 \rightarrow D_{s1}^{\prime-} \tau^+ \nu_\tau$
A_{FB}	This work [67]	$-0.407^{+0.104+0.129+0.020}_{-0.101-0.185-0.029}$ -0.41	$-0.405^{+0.104+0.129+0.020}_{-0.102-0.186-0.029}$ -0.40	$-0.248^{+0.026+0.080+0.048}_{-0.064-0.027-0.007}$ -0.20
Channels		$B^+ \rightarrow \bar{D}_1^0 e^+ \nu_e$	$B^+ \rightarrow \bar{D}_1^0 \mu^+ \nu_\mu$	$B^+ \rightarrow \bar{D}_1^0 \tau^+ \nu_\tau$
A_{FB}	This work	$-0.178^{+0.014+0.018+0.008}_{-0.030-0.025-0.017}$	$-0.177^{+0.012+0.016+0.006}_{-0.032-0.028-0.019}$	$-0.131^{+0.024+0.037+0.014}_{-0.034-0.036-0.025}$
Channels		$B^+ \rightarrow \bar{D}_1^{\prime 0} e^+ \nu_e$	$B^+ \rightarrow \bar{D}_1^{\prime 0} \mu^+ \nu_\mu$	$B^+ \rightarrow \bar{D}_1^{\prime 0} \tau^+ \nu_\tau$
A_{FB}	This work	$-0.316^{+0.115+0.085+0.083}_{-0.190-0.090-0.048}$	$-0.314^{+0.111+0.081+0.079}_{-0.096-0.095-0.043}$	$-0.186^{+0.013+0.041+0.024}_{-0.032-0.013-0.017}$

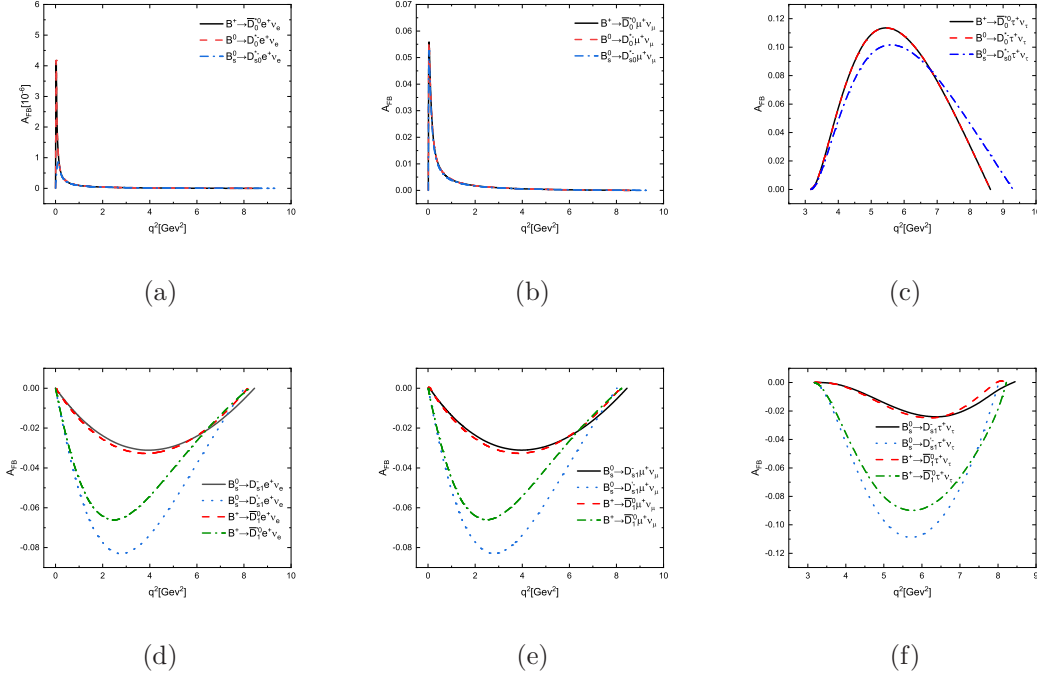


FIG. 6: The q^2 dependencies of the forward-backward asymmetries A_{FB} for the decays $B_{(s)} \rightarrow D_{(s)0}^* \ell \nu \ell$ and $B_{(s)} \rightarrow D_{(s)1}^{(\prime)} \ell \nu \ell$.

From Table VIII, we find that the ratios of the forward-backward asymmetries A_{FB}^μ/A_{FB}^e between the semileptonic decays $B_{(s)} \rightarrow D_{(s)0}^* \mu^+ \nu_\mu$ and $B_{(s)} \rightarrow D_{(s)0}^* e^+ \nu_e$ are about 3.5×10^4 . The reason is that the forward-backward asymmetries A_{FB} for the decays $B_{(s)} \rightarrow D_{(s)0}^* \ell^+ \nu_\ell$ are proportional to the square of the lepton mass. Undoubtedly, the effect of lepton mass can be well checked in such decay mode with a scalar meson involved in the final states. While for the decays $B_{(s)} \rightarrow D_{(s)1}^{(\prime)} \ell' \nu_{\ell'}$, the values of the forward-backward asymmetries A_{FB}^μ and A_{FB}^e are almost equal to each other. The magnitudes of the A_{FB} for the decays $B_{(s)} \rightarrow D_{(s)1}' \ell \nu_\ell$ are larger than those for the decays $B_{(s)} \rightarrow D_{(s)1} \ell \nu_\ell$. It is worth mentioning that our results are consistent well with those calculated in the nonrelativistic constituent quark models [67], which are shown in Table VIII. In Figure 6, we also display the q^2 -dependencies of the forward-backward asymmetries A_{FB} for the decays $B_{(s)} \rightarrow D_{(s)0}^* \ell \nu_\ell$ and $B_{(s)} \rightarrow D_{(s)1}^{(\prime)} \ell \nu_\ell$. Obviously, the signs of the A_{FB} for the decays $B_{(s)} \rightarrow D_{(s)0}^* \ell \nu_\ell$ are contrary with those for the decays $B_{(s)} \rightarrow D_{(s)1}^{(\prime)} \ell \nu_\ell$. The lepton mass effects can be easily observed in these figures.

IV. SUMMARY

In this work, we used the covariant light-front quark method to comprehensively investigate the semileptonic $B_{(s)}$ decays to D_0^* , D_{s0}^* , $D_{s1}^{(\prime)}$ and $D_1^{(\prime)}$, which can provide an important reference for future experiments. We calculated the branching ratios, the longitudinal polarization fractions f_L , and the forward-backward asymmetries A_{FB} for these semileptonic $B_{(s)}$ decays using the helicity amplitudes combined with form factors. We found the following points:

1. The small form factors of the transitions $B_{(s)} \rightarrow D_0^*, D_{s0}^*$ are related to the small decay constants $f_{D_0^*}$ and $f_{D_{s0}^*}$. Unfortunately, there are large uncertainties in these two decay constants. Combined with the data, our predictions for the branching ratios of the semileptonic $B_{(s)}$ meson decays with D_0^* and D_{s0}^* involved are helpful in probing the inner structures of these two resonances. Recently, Belle updated their measurement for the decays $B^0 \rightarrow D_0^{*-} \ell'^+ \nu_{\ell'}$ with only a small upper limit $Br(B^0 \rightarrow D_0^{*-} \ell'^+ \nu_{\ell'}) < 0.44 \times 10^{-3}$ obtained, which is much larger than most theoretical predictions. We urge our experimental colleagues to perform further more precise measurements to clarify this new puzzle.
2. In our considered decays, the branching ratios of the channels $B_s^0 \rightarrow D_{s1}^- \ell^+ \nu_\ell$ are (much) larger than those of the decays $B_s^0 \rightarrow D_{s1}' \ell^+ \nu_\ell$. This is because the related form factors of the transition $B_s \rightarrow D_{s1}$ are much larger than those of the transition

$B_s \rightarrow D'_{s1}$. There exists a similar situation between the decays $B^+ \rightarrow \bar{D}_1^0 \ell^+ \nu_\ell$ and $B^+ \rightarrow \bar{D}_1^0 \ell^+ \nu_\ell$. In addition, we calculated the dependencies of the branching ratios of the decays $B \rightarrow D_1^{(\prime)} \ell \nu_\ell$ and $B_s \rightarrow D_{s1}^{(\prime)} \ell \nu_\ell$ on the mixing angle θ_s . One can find that taking some negative mixing angle θ_s values within a range from -30.3° to -24.9° can explain the data, which correspond to θ within the range $5^\circ \sim 10.4^\circ$.

3. In these semileptonic decays $B_{(s)} \rightarrow D_{(s)1}^{(\prime)} \ell \nu_\ell$, the longitudinal polarization fractions in small q^2 region are always larger than those in large q^2 region. Furthermore, the longitudinal polarization for the decays with $D_{(s)1}$ involved in the final states is dominant, while it is contrary for the decays with $D'_{(s)1}$ involved. It is interesting that taking some special q^2 values for the decays $B \rightarrow D_1' \ell' \nu_{\ell'}$ and $B_s \rightarrow D_{s1}' \ell' \nu_{\ell'}$, we find that the contribution from the longitudinal polarization almost disappears with only the transverse polarizations left. Maybe such a phenomenon can be searched for in the future LHC and Super KEKB experiments to test the present mixing mechanism.

Acknowledgment

We thank Prof. Guo-Li Wang for helpful discussions. This work is partly supported by the National Natural Science Foundation of China under Grant No. 11347030, the Program of Science and Technology Innovation Talents in Universities of Henan Province 14HASTIT037, as well as the Natural Science Foundation of Henan Province under Grant No. 232300420116.

Appendix A: Some specific rules under the p^- intergration

When performing the integraion, we need to include the zero-mode contributions. It amounts to performing the integration in a proper way in the CLFQM. Specifically we use the following rules given in Refs. [41, 43]

$$\hat{p}'_{1\mu} \doteq P_\mu A_1^{(1)} + q_\mu A_2^{(1)}, \quad (\text{A1})$$

$$\hat{p}'_{1\mu} \hat{p}'_{1\nu} \doteq g_{\mu\nu} A_1^{(2)} + P_\mu P_\nu A_2^{(2)} + (P_\mu q_\nu + q_\mu P_\nu) A_3^{(2)} + q_\mu q_\nu A_4^{(2)}, \quad (\text{A2})$$

$$Z_2 = \hat{N}'_1 + m_1'^2 - m_2^2 + (1 - 2x_1) M'^2 + (q^2 + q \cdot P) \frac{\hat{p}'_\perp \cdot \hat{q}_\perp}{q^2}, \quad (\text{A3})$$

$$A_1^{(1)} = \frac{x_1}{2}, \quad A_2^{(1)} = A_1^{(1)} - \frac{\hat{p}'_\perp \cdot \hat{q}_\perp}{q^2}, \quad A_3^{(2)} = A_1^{(1)} A_2^{(1)}, \quad (\text{A4})$$

$$A_4^{(2)} = \left(A_2^{(1)} \right)^2 - \frac{1}{q^2} A_1^{(2)}, \quad A_1^{(2)} = -p_\perp'^2 - \frac{(\hat{p}'_\perp \cdot \hat{q}_\perp)^2}{q^2}, \quad A_2^{(2)} = \left(A_1^{(1)} \right)^2. \quad (\text{A5})$$

Appendix B: EXPRESSIONS OF $B \rightarrow D_0^*, {}^i D_1$ FORM FACTORS

$$F_1^{BD_0^*}(q^2) = \frac{N_c}{16\pi^3} \int dx_2 d^2 p'_\perp \frac{h'_B h''_{D_0^*}}{x_2 \hat{N}'_1 \hat{N}''_1} \left[x_1 (M_0'^2 + M_0''^2) + x_2 q^2 - x_2 (m'_1 + m''_1)^2 - x_1 (m'_1 - m_2)^2 - x_1 (m''_1 + m_2)^2 \right], \quad (\text{B1})$$

$$F_0^{BD_0^*}(q^2) = F_1^{BD_0^*}(q^2) + \frac{q^2}{q \cdot P} \frac{N_c}{16\pi^3} \int dx_2 d^2 p'_\perp \frac{2h'_B h''_{D_0^*}}{x_2 \hat{N}'_1 \hat{N}''_1} \left\{ -x_1 x_2 M'^2 - p_\perp'^2 - m'_1 m_2 - (m''_1 + m_2)(x_2 m'_1 + x_1 m_2) + 2 \frac{q \cdot P}{q^2} \left(p_\perp'^2 + 2 \frac{(p'_\perp \cdot q_\perp)^2}{q^2} \right) + 2 \frac{(p'_\perp \cdot q_\perp)^2}{q^2} - \frac{p'_\perp \cdot q_\perp}{q^2} [M''^2 - x_2 (q^2 + q \cdot P) - (x_2 - x_1) M'^2 + 2x_1 M_0'^2 - 2(m'_1 - m_2)(m'_1 - m''_1)] \right\}, \quad (\text{B2})$$

$$A^{B {}^i D_1}(q^2) = (M' - M'') \frac{N_c}{16\pi^3} \int dx_2 d^2 p'_\perp \frac{2h'_B h''_{D_1}}{x_2 \hat{N}'_1 \hat{N}''_1} \left\{ x_2 m'_1 + x_1 m_2 + (m'_1 + m''_1) \frac{p'_\perp \cdot q_\perp}{q^2} + \frac{2}{w''_{D_{s1}}} \left[p_\perp'^2 + \frac{(p'_\perp \cdot q_\perp)^2}{q^2} \right] \right\}, \quad (\text{B3})$$

$$V_1^{B {}^i D_1}(q^2) = -\frac{1}{M' - M''} \frac{N_c}{16\pi^3} \int dx_2 d^2 p'_\perp \frac{h'_B h''_{D_1}}{x_2 \hat{N}'_1 \hat{N}''_1} \left\{ 2x_1 (m_2 - m'_1) (M_0'^2 + M_0''^2) + 4x_1 m''_1 M_0'^2 + 2x_2 m'_1 q \cdot P + 2m_2 q^2 - 2x_1 m_2 (M'^2 + M''^2) + 2(m'_1 - m_2)(m'_1 - m''_1)^2 + 8(m'_1 - m_2) \times \left[p_\perp'^2 + \frac{(p'_\perp \cdot q_\perp)^2}{q^2} \right] + 2(m'_1 - m''_1)(q^2 + q \cdot P) \frac{p'_\perp \cdot q_\perp}{q^2} - 4 \frac{q^2 p_\perp'^2 + (p'_\perp \cdot q_\perp)^2}{q^2 w''_{D_{s1}}} \times \left[2x_1 (M'^2 + M_0'^2) - q^2 - q \cdot P - 2(q^2 + q \cdot P) \frac{p'_\perp \cdot q_\perp}{q^2} - 2(m'_1 + m''_1)(m'_1 - m_2) \right] \right\}, \quad (\text{B4})$$

$$V_2^{B {}^i D_1}(q^2) = (M' - M'') \frac{N_c}{16\pi^3} \int dx_2 d^2 p'_\perp \frac{2h'_B h''_{D_1}}{x_2 \hat{N}'_1 \hat{N}''_1} \left\{ (x_1 - x_2)(x_2 m'_1 + x_1 m_2) - [2x_1 m_2 - m''_1 + (x_2 - x_1) m'_1] \times \frac{p'_\perp \cdot q_\perp}{q^2} - 2 \frac{x_2 q^2 + p'_\perp \cdot q_\perp}{x_2 q^2 w''_{D_1}} [p'_\perp \cdot p''_\perp + (x_1 m_2 + x_2 m'_1) \times (x_1 m_2 + x_2 m''_1)] \right\}, \quad (\text{B5})$$

$$V_0^{B {}^i D_1}(q^2) = \frac{M' - M''}{2M''} V_1^{B {}^i D_1}(q^2) - \frac{M' + M''}{2M''} V_2^{B {}^i D_1}(q^2) - \frac{q^2}{2M''} \frac{N_c}{16\pi^3} \int dx_2 d^2 p'_\perp \frac{h'_B h''_{D_1}}{x_2 \hat{N}'_1 \hat{N}''_1} \times \left\{ 2(2x_1 - 3)(x_2 m'_1 + x_1 m_2) - 8(m'_1 - m_2) \left[\frac{p_\perp'^2}{q^2} + 2 \frac{(p'_\perp \cdot q_\perp)^2}{q^4} \right] - [(14 - 12x_1) m'_1 + 2m''_1 - (8 - 12x_1) m_2] \frac{p'_\perp \cdot q_\perp}{q^2} + \frac{4}{w''_{D_1}} ([M'^2 + M''^2 - q^2 + 2(m'_1 - m_2)(-m''_1 + m_2)] \times (A_3^{(2)} + A_4^{(2)} - A_2^{(1)}) + Z_2 (3A_2^{(1)} - 2A_4^{(2)} - 1) + \frac{1}{2} [x_1 (q^2 + q \cdot P) - 2M'^2 - 2p'_\perp \cdot q_\perp - 2m'_1 (-m''_1 + m_2) - 2m_2 (m'_1 - m_2)]) (A_1^{(1)} + A_2^{(1)} - 1) \times q \cdot P \left[\frac{p_\perp'^2}{q^2} + \frac{(p'_\perp \cdot q_\perp)^2}{q^4} \right] (4A_2^{(1)} - 3) \right\}, \quad (\text{B6})$$

with $i = 1, 3$.

-
- [1] Z. H. Wang, Y. Zhang, T. h. Wang, Y. Jiang, Q. Li and G. L. Wang, *Chin. Phys. C* **42**, 123101 (2018) [arXiv:1803.06822 [hep-ph]].
 - [2] K. Abe, *et al.* [Belle], *Phys. Rev. D* **69**, 112002 (2004) [arXiv:hep-ex/0307021].
 - [3] S. Godfrey and N. Isgur, *Phys. Rev. D* **32**, 189 (1985).
 - [4] B. Aubert, *et al.* [BaBar] , *Phys. Rev. D* **79**, 112004 (2009) [arXiv:hep-ex/0901.1291].
 - [5] S. Godfrey and R. Kokoski, *Phys. Rev. D* **43**, 1679 (1991).
 - [6] N. Gubernari, A. Khodjamirian, R. Mandal and T. Mannel, *JHEP* **05**, 029 (2022) [arXiv:2203.08493 [hep-ph]].
 - [7] V. Morenas, A. Le Yaouanc, L. Oliver, O. Pene and J. C. Raynal, *Phys. Rev. D* **56**, 5668 (1997) [arXiv:hep-ph/9706265].
 - [8] I. I. Bigi, B. Blossier, A. Le Yaouanc, L. Oliver, O. Pene, J. C. Raynal, A. Oyanguren and P. Roudeau, *Eur. Phys. J. C* **52**, 975 (2007) [arXiv:0708.1621 [hep-ph]].
 - [9] D. Scora and N. Isgur, *Phys. Rev. D* **52**, 2783 (1995) [arXiv:hep-ph/9503486].
 - [10] P. Colangelo, F. De Fazio and N. Paver, *Phys. Rev. D* **58**, 116005 (1998) [arXiv:hep-ph/9804377].
 - [11] F.Meier *et al.* [Belle], *Phys. Rev. D* **107**, 092003 (2023) [arXiv:2211.09833 [hep-ex]].
 - [12] Z. X. Xie, G. Q. Feng and X. H. Guo, *Phys. Rev. D* **81**, 036014 (2010).
 - [13] M. Cleven, H. W. Griehammer, F. K. Guo, C. Hanhart and U. G. Meiner, *Eur. Phys. J. A* **50**, 149 (2014) [arXiv:1405.2242 [hep-ph]].
 - [14] F. K. Guo, P. N. Shen, H. C. Chiang, R. G. Ping and B. S. Zou, *Phys. Lett. B* **641**, 278 (2006) [arXiv:hep-ph/0603072].
 - [15] T. Barnes, F. E. Close and H. J. Lipkin, *Phys. Rev. D* **68**, 054006 (2003) [arXiv:hep-ph/0305025].
 - [16] E. E. Kolomeitsev and M. F. M. Lutz, *Phys. Lett. B* **582**, 39 (2004) [arXiv:hep-ph/0307133].
 - [17] J. Hofmann and M. F. M. Lutz, *Nucl. Phys. A* **733**, 142 (2004) [arXiv:hep-ph/0308263].
 - [18] C. J. Xiao, D. Y. Chen and Y. L. Ma, *Phys. Rev. D* **93**, 094011 (2016) [arXiv:1601.06399 [hep-ph]].
 - [19] L. Maiani, F. Piccinini, A. D. Polosa and V. Riquer, *Phys. Rev. D* **71**, 014028 (2005) [arXiv:hep-ph/0412098].
 - [20] Z. G. Wang and S. L. Wan, *Nucl. Phys. A* **778**, 22 (2006) [arXiv:hep-ph/0602080].
 - [21] H. Y. Cheng and W. S. Hou, *Phys. Lett. B* **566**, 193 (2003) [arXiv:hep-ph/0305038].

- [22] Y. Q. Chen and X. Q. Li, Phys. Rev. Lett. **93**, 232001 (2004) [arXiv:hep-ph/0407062].
- [23] H. Kim and Y. Oh, Phys. Rev. D **72**, 074012 (2005) [arXiv:hep-ph/0508251].
- [24] W. A. Bardeen, E. J. Eichten and C. T. Hill, Phys. Rev. D **68**, 054024 (2003) [arXiv:hep-ph/0305049].
- [25] M. A. Nowak, M. Rho and I. Zahed, Acta Phys. Polon. B **35**, 2377 (2004) [arXiv:hep-ph/0307102].
- [26] T. E. Browder, S. Pakvasa and A. A. Petrov, Phys. Lett. B **578**, 365 (2004) [arXiv:hep-ph/0307054].
- [27] J. Vijande, F. Fernandez and A. Valcarce, Phys. Rev. D **73**, 034002 (2006) [arXiv:hep-ph/0601143].
- [28] H. Y. Cheng, Phys. Rev. D **68**, 094005 (2003) [arXiv:hep-ph/0307168].
- [29] H. Y. Cheng, C. K. Chua and C. W. Hwang, Phys. Rev. D **69**, 074025 (2004) [arXiv:hep-ph/0310359].
- [30] Y. B. Dai and M. Q. Huang, Phys. Rev. D **59**, 034018 (1999) [arXiv:hep-ph/9807461].
- [31] M. Q. Huang and Y. B. Dai, Phys. Rev. D **64**, 014034 (2001) [arXiv:hep-ph/0102299].
- [32] Y. B. Zuo, H. Y. Jin, J. Y. Tian, J. Yi, H. Y. Gong and T. T. Pan, Chin. Phys. C **47**, 103104 (2023) [arXiv:2307.08271 [hep-ph]].
- [33] A. K. Leibovich, Z. Ligeti, I. W. Stewart and M. B. Wise, Phys. Rev. Lett. **78**, 3995 (1997) [arXiv:hep-ph/9703213].
- [34] A. K. Leibovich, Z. Ligeti, I. W. Stewart and M. B. Wise, Phys. Rev. D **57**, 308 (1998) [arXiv:hep-ph/9705467].
- [35] F. U. Bernlochner, Z. Ligeti and D. J. Robinson, Phys. Rev. D **97**, 075011 (2018) [arXiv:1711.03110 [hep-ph]].
- [36] F. U. Bernlochner and Z. Ligeti, Phys. Rev. D **95**, 014022 [arXiv:1606.09300 [hep-ph]].
- [37] H. Y. Cheng and C. K. Chua, Phys. Rev. D **69**, 094007 (2004) [erratum: Phys. Rev. D **81**, 059901 (2010)] [arXiv:hep-ph/0401141].
- [38] C. W. Hwang and Z. T. Wei, J. Phys. G **34**, 687 (2007) [arXiv:hep-ph/0609036].
- [39] C. D. Lu, W. Wang and Z. T. Wei, Phys. Rev. D **76**, 014013 (2007) [arXiv:hep-ph/0701265].
- [40] W. Wang, Y. L. Shen and C. D. Lu, Eur. Phys. J. C **51**, 841 (2007) [arXiv:hep-ph/0704.2493].
- [41] W. Jaus, Phys. Rev. D **60**, 054026 (1999).
- [42] M. Wirbel, B. Stech and M. Bauer, Z. Phys. C **29**, 637 (1985).
- [43] H. Y. Cheng, C. K. Chua and C. W. Hwang, Phys. Rev. D **69**, 074025 (2004) [arXiv:hep-ph/0310359].
- [44] Z. Q. Zhang, Z. J. Sun, Y. C. Zhao, Y. Y. Yang and Z. Y. Zhang, Eur. Phys. J. C **83**, 477

- (2023) [arXiv:2301.11107 [hep-ph]].
- [45] Y. Sakaki, M. Tanaka, A. Tayduganov and R. Watanabe, Phys. Rev. D **88**, 094012 (2013) [arXiv:1309.0301 [hep-ph]].
- [46] M. Beneke and M. Neubert, Nucl. Phys. B **675**, 333 (2003) [arXiv:hep-ph/0308039].
- [47] S. Navaset *et al.* [Particle Data Group], Phys. Rev. D **110**, 030001 (2024).
- [48] D. Becirevic, P. Boucaud, J. P. Leroy, V. Lubicz, G. Martinelli, F. Mescia and F. Rapuano, Phys. Rev. D **60**, 074501 (1999) [arXiv:hep-lat/9811003].
- [49] H. Y. Cheng, Phys. Rev. D **68**, 094005 (2003) [arXiv:hep-ph/0307168].
- [50] R. H. Li and C. D. Lu, Phys. Rev. D **80**, 014005 (2009) [arXiv:0905.3259 [hep-ph]].
- [51] W. Y. Wang, J. Phys. G **37**, 045006 (2010) [arXiv:1101.0249 [hep-ph]].
- [52] X. W. Kang, T. Luo, Y. Zhang, L. Y. Dai and C. Wang, Eur. Phys. J. C **78**, 909 (2018) [arXiv:1808.02432 [hep-ph]].
- [53] N. Gubernari, A. Khodjamirian, R. Mandal and T. Mannel, JHEP **12**, 015 (2023) [arXiv:2309.10165 [hep-ph]].
- [54] Y. L. Shen, Z. J. Yang and X. Yu, Phys. Rev. D **90**, 114015 (2014) [arXiv:1207.5912 [hep-ph]].
- [55] D. Liventsev *et al.* [Belle], Phys. Rev. D **77**, 091503 (2008) [arXiv:0711.3252 [hep-ex]].
- [56] F. Meier *et al.* [Belle], Phys. Rev. D **107**, 092003 (2023) [arXiv:2211.09833 [hep-ex]].
- [57] B. Aubert *et al.* [BaBar], Phys. Rev. Lett. **101**, 261802 (2008) [arXiv:0808.0528 [hep-ex]].
- [58] A. L. Yaouanc, J. P. Leroy and P. Roudeau, Phys. Rev. D **105**, 013004 (2022) [arXiv:2102.11608 [hep-ph]].
- [59] F. S. Navarra, M. Nielsen, E. Oset and T. Sekihara, Phys. Rev. D **92**, 014031 (2015) [arXiv:1501.03422 [hep-ph]].
- [60] S. M. Zhao, X. Liu and S. J. Li, Eur. Phys. J. C **51**, 601 (2007) [arXiv:hep-ph/0612008].
- [61] T. M. Aliev, K. Azizi and A. Ozpineci, Eur.Phys. J. C **51**, 593 (2007) [arXiv:hep-ph/0608264].
- [62] R. N. Faustov and V. O. Galkin, Phys. Rev. D **87**, 034033 (2013) [arXiv:1212.3167 [hep-ph]].
- [63] R. C. Verma, J. Phys. G **39**, 025005 (2012) [arXiv:1103.2973 [hep-ph]].
- [64] M. Q. Huang, Phys. Rev. D **69**, 114015 (2004) [arXiv:hep-ph/0404032].
- [65] T. M. Aliev and M. Savci, Phys. Rev. D **73**, 114010 (2006) [arXiv:hep-ph/0604002].
- [66] W. Y. Wang and Y. L. Wu, Int. J. Mod. Phys. A **16**, 2505 (2001) [arXiv:hep-ph/0012240].
- [67] C. Albertus, Phys. Rev. D **89**, 065042 (2014) [arXiv:1401.1791 [hep-ph]].